

Ice core evidence for a 20th century increase in surface mass balance in coastal Dronning Maud Land, East Antarctica

Morgane Philippe¹, Jean-Louis Tison¹, Karen Fjøsne¹, Bryn Hubbard², Helle A. Kjær³, Jan T. M. Lenaerts⁴, Reinhard Drews⁵, Simon G. Sheldon³, Kevin De Bondt⁶, Philippe Claeys⁶,
5 Frank Pattyn¹

¹Laboratoire de Glaciologie, Département des Géosciences, Environnement et Société, Université Libre de Bruxelles, BE-1050 Brussels, Belgium

²Centre for Glaciology, Department of Geography and Earth Sciences, Aberystwyth University SY23 3DB, United Kingdom

10 ³Centre for ice and climate, Niels Bohr Institute, University of Copenhagen, Juliane Maries Vej 30, 2100, Copenhagen, Denmark

⁴Institute for Marine and Atmospheric research Utrecht, Utrecht University, Princetonplein 5, 3584 CC Utrecht, Netherlands

⁵Bavarian Academy for Sciences and Humanities, Alfons-Goppel-Strasse 11, 80539 Munich, Germany

15 ⁶Department of Analytical Environmental and Geo-Chemistry, Vrije Universiteit Brussel, Pleinlaan 2, BE-1050 Brussels, Belgium

Correspondence to: M. Philippe (mophilip@ulb.ac.be)

Abstract. Ice cores provide temporal records of Surface Mass Balance (SMB), a crucial component of Antarctic mass balance. Coastal areas have relatively high and sensitive SMN but are under-represented in records
20 spanning more than 100 years. Here we present records from a 120 m ice core drilled on the Derwael Ice Rise, coastal Dronning Maud Land (DML), East Antarctica in 2012. Water stable isotopes ($\delta^{18}\text{O}$ and δD) stratigraphy is supplemented by discontinuous major ion profiles and continuous electrical conductivity measurements (ECM). The ice core bottom is dated back to 1759 ± 16 A.D. The resulting annual layer thickness history is
25 combined with the gravimetric density profile to reconstruct SMB history, corrected for the influence of ice deformation. The mean long-term SMB is 0.47 ± 0.02 m water equivalent (w.e.) a^{-1} . Reconstructed annual SMB show an increase in at least the last 50 years to a mean value of 0.61 ± 0.01 m w.e. a^{-1} between 1962 and 2011. This trend is compared with other reported SMB data in Antarctica, generally showing a high spatial variability. Output of the fully coupled Community Earth System Model suggests that, although atmospheric circulation is the main factor influencing SMB, variability in sea surface temperatures and sea ice cover in the precipitation
30 source region also explain part of the variability in SMB, along with local snow redistribution. The latter likely has a significant impact on interannual variability but not on long-term trends. This is the first record from a coastal ice core in East Antarctica showing a steady increase of SMB during the 20th and 21st centuries.

1 Introduction

In a changing climate, it is important to know the Surface Mass Balance (SMB, i.e. precipitation minus evaporation, sublimation, meltwater runoff, and/or erosion) of Earth's ice sheets as it is an essential component of their total mass balance, directly affecting sea level (Rignot et al., 2011). The average rate of Antarctic contribution to sea level rise is estimated to have increased from 0.08 [−0.10 to 0.27] mm a^{−1} for 1992–2001 to 0.40 [0.20 to 0.61] mm a^{−1} for 2002–2011, mainly due to increasing ice discharge from coastal West Antarctica (Vaughan et al., 2013), where the present-day warming seems to be confined (Turner et al., 2005; Bromwich et al., 2014; Ludescher et al., 2015).

Some studies suggested that this increase in dynamic ice loss could be partly balanced by a warming-related increase in precipitation (e.g. Krinner et al., 2007, Palerme et al., 2016) by the end of the 21st century, but this is subject to debate. For example, Frieler et al. (2015) showed that past Antarctic SMB were positively correlated with past air temperature during glacial–interglacial changes, using ice core data and modelling. However, Fudge et al. (2016) found that SMB and temperature are not always positively correlated in West Antarctica. There has been no significant long-term trend in the SMB over the continent during the past few decades (Van de Berg et al., 2006; Monaghan et al., 2006; van den Broeke et al., 2006; Bromwich et al., 2011; Lenaerts et al., 2012; Wang et al., 2016).

In East Antarctica, satellite radar and laser altimetry suggest recent mass gain (Shepherd et al., 2012). Dronning Maud Land (DML) in particular, has experienced several high SMB years since 2009 (Boening et al., 2012; Lenaerts et al., 2013). Calibrated regional atmospheric climate model indicate higher SMB during 1980–2004 along the coastal sectors (e.g. Van de Berg et al., 2006) and Wang et al. (2016) found that climate models generally underestimate SMB in coastal DML. This region is therefore of particular interest.

Ice cores provide temporal records of SMB, which are essential to calibrate internal reflection horizons in radio-echo sounding records (e.g. Fujita et al., 2011; Kingslake et al., 2014), to force ice sheet flow and dating models (e.g. Parenin et al., 2007) and to evaluate regional climate models (e.g. Lenaerts et al., 2014). However, records of SMB are still scarce relative to the size of Antarctica. While the majority show no significant trend in SMB over the last century (e.g. Nishio et al., 2002), some show an increase (e.g. Karlof et al., 2005), and others show a decrease (e.g. Kaczmarek et al., 2004). Frezzotti et al. (2013) compiled SMB records for the whole of Antarctica and Altnau et al. (2015) for DML more specifically. Frezzotti et al. (2013) showed no significant SMB changes over most of Antarctica since the 1960s, except for an increase in coastal regions with high SMB and in the highest part of the East Antarctic ice divide. Altnau et al. (2015) found a statistically significant positive trend in SMB for the interior DML and a negative trend at the coast.

However, there is still a clear need for data from the coastal areas of East Antarctica (ISMALSS Committee, 2004; van de Berg et al., 2006; Magand et al., 2007; Wang et al., 2016), where few studies focused on ice cores spanning more than 100 years. Coastal regions allow higher temporal resolution than the interior as SMB generally decrease with both elevation and distance from the coast (Frezzotti et al., 2005). Ice rises are ideal locations for paleoclimate studies (Matsuoka et al., 2015) as they are undisturbed by up-stream topography, and lateral flow is almost negligible. Melt events are also likely to be much less frequent than on ice shelves (Hubbard et al., 2013).

In this paper we report on water stable isotopes ($\delta^{18}\text{O}$ and δD) measurements (5–10 cm resolution) along a 120 m ice core drilled on the Derwael Ice Rise (DIR) in coastal DML. This record is complemented by major ion and continuous electrical conductivity measurement (ECM) profiles to improve the resolution of the seasonal cycles wherever necessary. After correcting for dynamic vertical thinning, we derive annual SMB, and average SMB and trends over the last 254 ± 16 years, i.e. across the Anthropocene transition. These are compared with other reported trends in Antarctica, including DML, over the last decades.

2 Field site and methods

2.1 Field site

The study site is located in coastal DML, East Antarctica. A 120 m ice core, named IC12 after the project name IceCon, was drilled in 2012 on the divide of the DIR ($70^{\circ}14'44.88''\text{S}$, $26^{\circ}20'5.64''\text{E}$, 450 m a.s.l., Fig. 1). This ice rise is 550 m thick and the recent SMB has been estimated to $0.50 \text{ m w.e. a}^{-1}$ from preliminary ice core analysis (Drews et al., 2015; Callens et al., 2016).

Ice rises provide scientifically valuable drill sites because they are located close to the ocean (and hence sample coastal precipitation regimes) and because ground-penetrating radar data can easily identify drill sites on a local dome that are relatively undisturbed by horizontal flow. However, a number of regional factors complicate the interpretation of ice-core records on ice rises: ice rises form topographic barriers with the capacity to disrupt atmospheric circulation on otherwise flat ice shelves. Orographic precipitation can thereby result in significantly high SMB values on the upwind sides of such ice rises, with corresponding precipitation shadows on the downwind side (Lenaerts et al., 2014). For the DIR in particular, the SMB on the upwind side is up to 2.5 times higher than on the downwind side (Callens et al., 2016). On top of this larger scale ($\sim 10 \text{ km}$) asymmetry, Drews et al. (2015) identified a small scale (km) SMB oscillation near the divide, tentatively attributed to erosion at the crest, and subsequent redeposition on its downwind side. The observed SMB maximum is therefore offset by ~ 4

km from the topographic divide where the ice core was drilled. This means that the absolute values of the ice-core derived SMB sample a regime where the SMB varies on short spatial scales. Moreover, Drews et al. (2015) identified isochrone arches (a.k.a. Raymond Bumps) beneath the divide. This characteristic flow pattern causes ice at shallow to intermediate depths beneath the divide to be older than at comparable depths in the ice-rise flanks, necessitating a specific strain correction for the ice-core analysis, which we discuss below. Both Drews et al. (2015) and Callens et al. (2016) suggested that the DIR has maintained its local ice divide for the last thousands of years and possibly longer. By matching the radar stratigraphy to an ice-flow model, Drews et al. (2015) suggested that the DIR divide elevation is close to steady-state and has potentially undergone modest surface lowering in the past. Both studies used a temporally constant SMB. Here we focus on the temporal variability and argue that, because the DIR has been stable in the past, we can draw conclusion with respect to the larger-scale atmospheric circulation patterns.

2.2 Ice coring and density analyses

The IC12 ice core was drilled with an Eclipse electromechanical ice corer in a dry borehole. The mean length of the core sections recovered after each run was 0.77 m and the standard deviation 0.40 m. The ice core is complete, except for the 100-101 m section, which fell back in the borehole and was recovered in broken pieces. Immediately after drilling, temperature (Testo 720 probe, inserted in a 4 mm diameter hole drilled to the centre of the core, precision ± 0.1 °C) and length were measured on each core section, which was then wrapped in a PVC bag, stored directly in a refrigerated container at -25 °C, and kept at this temperature until analysis at the home laboratory. The core sections were then bisected lengthwise, in a cold room at -20 °C. One half of the core section was used for ECM measurements and then kept as archive, and the other half was sectioned for water stable isotope sampling and major ion analysis. Only a few very thin (1 mm) ice layers are present. A best-fit through discrete gravimetric density measurements, previously published (Hubbard et al., 2013), is used here to convert measured annual layer thicknesses to meters water equivalent (w.e.) (Sect. 2.3).

2.3 Annual layer counting and dating

2.3.1 Water stable isotopes and major ion

Half of each core section was resampled as a central bar of 30 mm x 30 mm square section with a clean band saw. The outer part of the half-core was melted and stored in 4 ml bottles for $\delta^{18}\text{O}$ and δD measurements, completely filled to prevent contact with air. For major ion measurements, the inner bar was placed in a Teflon holder and further decontaminated by removing ~2 mm from each face under a class-100 laminar flow hood,

using a methanol-cleaned microtome blade. Each 5 cm long decontaminated section was then covered with a clean PE storage bottle, and the sample cut loose from the bar by striking it perpendicular to the bar axis. Blank ice samples prepared from milliQ water were processed before every new core section and analysed for contamination.

- 5 Dating was achieved by annual layer counting identified from the stratigraphy of the $\delta^{18}\text{O}$ and δD isotopic composition of H_2O measured with a PICARRO L 2130-i Cavity Ring Down Spectrometer (CRDS) (precision, $\sigma = 0.05 \text{ ‰}$ for $\delta^{18}\text{O}$ and 0.3 ‰ for δD). This composition was measured at 10 cm resolution in the top 80 m and 5 cm resolution below (See Fig. S1 for exact resolution). For sections of unclear isotopic seasonality, major ion analysis (Na^+ , Cl^- , SO_4^{2-} , NO_3^- and methylsulphonic acid (MSA)) was additionally carried out using a Dionex-
- 10 ICS5000 liquid chromatograph, at 5 cm resolution. The system has a standard deviation of 2 ppb for Na^+ and SO_4^{2-} , 8 ppb for Cl^- , 7 ppb for NO_3^- , and 1 ppb for MSA. Non sea-salt sulfate was calculated as $nss\text{SO}_4 = [\text{SO}_4^{2-}]_{\text{tot}} - 0.052 * [\text{Cl}^-]$, following Mulvaney et al. (1992) and represents all SO_4^{2-} not of a marine aerosol origin. The ratio $\text{Na}^+/\text{SO}_4^{2-}$ was also calculated as an indicator of seasonal SO_4^{2-} production.

2.3.2 ECM measurements

- 15 ECM measurements were carried out in a cold room at -18°C at the Centre for Ice and Climate, Niels Bohr Institute, University of Copenhagen, with a modified version of the Copenhagen ECM described by Hammer (1980). Direct current (1250 V) was applied at the surface of the freshly-cut ice and electrical conductivity was measured at 1 mm resolution. The DC electrical conductivity of the ice, once corrected for temperature, depends principally on its acidity (Hammer, 1980; Hammer et al., 1994). This content varies seasonally and usually
- 20 shows longer term localized maxima associated with sulfate production from volcanic eruptions. ECM can therefore be used both as a relative and an absolute dating tool.

- As measurements were principally made in firn, we applied a novel technique described by Kjær et al. (in review) to correct for the effect of the firn porosity on the amplitude of the signal. As the ECM current is low for higher air content, we multiplied the high resolution ECM signal by the inverse of the ice volume fraction, i.e.
- 25 the ratio of the ice density to firn density ($\rho_{\text{ice}}/\rho_{\text{firn}}$), using the gravimetric density best fit from Hubbard et al. (2013).

- ECM data were smoothed with a 301 point first-order Savitsky–Golay filter (Savitsky and Golay, 1964) which eliminates peaks due to random noise and small-scale variations in material chemical composition while preserving the larger peaks, including those due to volcanic eruptions. Finally, the ECM data were normalized by
- 30 subtracting the mean and dividing by the standard deviation following Karlof et al. (2000).

2.4. Corrections for ice flow

The compression of snow under its own weight not only involves density changes along the vertical, but also involves lateral deformation of the underlying ice. Failure to take the latter process into account would provide an underestimation of reconstructed initial annual layer thickness, and therefore of the SMB, especially within the oldest part of the record. In this paper, two different models are used to represent vertical strain rate evolution with depth: (i) strain rates derived from a full Stokes model that represent the full Raymond effect measured at the ice divide (Drews et al., 2015); and (ii) a modified Dansgaard–Johnsen model (Dansgaard and Johnsen, 1969) based on the description given in Cuffey and Paterson (2010).

The Drews et al. (2015) strain rate profile accounts for the best fit with the radar layers at depth, taking into account a small amount of surface thinning (0.03 m a^{-1}) and anisotropy (although the former is not essential). From a hexagonal strain network, we calculated horizontal strain rates ($\epsilon_{xx} + \epsilon_{yy}$) to be 0.002 a^{-1} . Mass conservation then gives a vertical strain rate at the surface of -0.002 a^{-1} . The vertical velocity profile was then scaled to match this measured value. A best fit to the measured radar layers was obtained with a value of a mean SMB of 0.55 m a^{-1} ice equivalent (Fig. 2).

Alternatively, we used the Dansgaard–Johnsen (D–J) model to fit the characteristics at the ice divide, exhibited by the Raymond effect. Assuming that the horizontal velocity is zero, the vertical velocity is maximum at the surface and equals the SMB (with negative sign) and is zero at the bed. Assuming a vertical strain rate of -0.002 a^{-1} at the surface, we can determine the kink point (between constant strain rate above and a strain rate linearly decreasing with depth below) that obeys these conditions (Cuffey and Paterson, 2010). This approach indicates that the kink point lies at $0.9H$, where H is the ice thickness. As seen in Fig. 2b, this method yields a vertical strain pattern that is consistent with that of Drews et al. (2015), especially in the first 120 m corresponding to the length of the ice core.

Both strain rates (Drews/D–J) were then used to correct the ice equivalent annual layer thickness for strain thinning. Annual layer thicknesses were then converted from ice equivalent to w.e. for easier comparison with other studies.

2.5 Community Earth System Model (CESM)

Atmospheric reanalyses and regional climate models extend back to 1979, which means that they cover only a small proportion of the ice core record. Instead, to interpret our ice core derived SMB record and relate it to the large-scale climate conditions, we use output from the Community Earth System Model (CESM). CESM is a global, fully coupled, CMIP6-generation climate model with an approximate horizontal resolution of 1° , and has

recently been used successfully to simulate present-day Antarctic climate and SMB (Lenaerts et al., 2016). We use the historical time series of CESM (156 years, 1850–2005) that overlaps with most of the ice core record, and group the 16 single years (i.e. ~10 %) with the highest SMB and lowest SMB in that time series. We take the mean SMB of the ice covered CESM grid points of the coastal region around the ice core (20–30 °E, 69–72
5 °S) as a representative value. For the grouped years of highest and lowest SMB, we take the anomalies (relative to the 1850–2005 mean) in near-surface temperature and sea-ice fraction as parameters to describe the regional ocean and atmosphere conditions corresponding to these extreme years. The CESM simulated sea-ice extent in the observational period is very realistic compared to observations (Lenaerts et al., 2016) and does not show any trend in the Atlantic sector, which gives us confidence that the sea ice is treated realistically.

10 3 Results

3.1 Dating

3.1.1 Relative dating (seasonal peak counting)

Figures 3, S1 and S2 illustrate how the high-resolution water stable isotopes ($\delta^{18}\text{O}$, δD), smoothed ECM, chemical species and their ratios are used in combination to identify annual layer boundaries. All of these
15 physico-chemical variables generally show a clear seasonality, undisturbed by the few very thin ice layers (white dots in Fig. 3). The summer peak in water stable isotopes is obvious in most cases. The boundary between annual layers was identified as the middle depth of the peak above the mean $\delta^{18}\text{O}$ value (thin black line in Fig. 3), considered as the “summer season”. Major ion such as nssSO_4 , NO_3^- , and especially the ratio $\text{Na}^+/\text{SO}_4^-$ generally help to distinguish ambiguous peaks in the isotopic record. SO_4^- is one of the oxidation products of
20 Dimethyl Sulfide (DMS), a degradation product of DMSP (dimethylsulfoniopropionate) which is synthesized by sea ice microorganisms (sympagic) as an antifreeze and osmotic regulator (e.g. Levasseur, 2013). Both nssSO_4 and $\text{Na}^+/\text{SO}_4^-$ vary seasonally. NO_3^- also shows a seasonal signal, but the processes controlling its seasonality are not yet fully understood (Wolff et al., 2008). For ECM, there is also a regular seasonal signal, which is sometimes blurred below 80 m, although some seasonal cycles can still be seen, for example between 115 and
25 118 m. (Fig. S2). Two extreme age–depth profiles (youngest and oldest) resulted from this counting procedure, taking the remaining ambiguities into account (Fig. S2). The mean age–depth profile is presented in Fig. 4 with the ranges associated with the two extreme age–depth estimates. Between 237 and 269 annual cycles were identified between the reference surface (2012 A.D.) and the bottom of the core, which is consequently dated to 1759 ± 16 A.D..

In the oldest estimate, each $\text{Na}^+/\text{SO}_4^-$ can generally be associated with a trough in $\delta^{18}\text{O}$, even in the deep parts of the record. This is the case between 101 and 110 m or between 112 and 115 m, for example (Fig. S2), while in the youngest estimate, these years show a double peak in $\text{Na}^+/\text{SO}_4^-$, suggesting the latter underestimates the number of years. We will now see if we can find a confirmation for trusting this oldest estimate from volcanic signals in the ECM record.

3.1.2 Can we identify volcanic horizons to refine our depth-age scale?

Volcanic indicators (ECM, nssSO_4 , $\text{SO}_4^-/\text{Na}^+$) can be used to identify specific, dated volcanic eruptions, allowing us to reduce the uncertainties resulting from the relative dating procedure. However, unambiguous eruption identifications are challenging in ice cores from coastal regions, where the ECM and nssSO_4 background signals are commonly highly variable due to the proximity of the ocean and ocean-related MSA products (Fig. S1).

Given the preliminary dating of 1759 ± 16 A.D. made on the basis of our relative core dating (Section 3.1.1 above), we have looked for volcanic horizons at the depths corresponding to the oldest estimate to try and refine this timescale (Figure 5). The Tambora eruption seems to appear at 102.35 m, with an ECM signature above the 4σ threshold and a consecutive peak above the 2σ threshold, which could be attributed to the 1809 eruption (unknown volcano, Traufetter et al., 2004). Although this is much less pronounced than in other cores, more inland, such as WAIS divide (Sigl et al., 2013), this threshold is usually considered as sufficient (e.g. Kaczmarek et al., 2004) and allows potential matching of 13 volcanoes. However, many other peaks above that threshold could not be associated with any known volcanic eruption. Therefore, we concluded that the background is too noisy to refine the relative time scale in this core. As a result, we will keep both estimates resulting from our relative dating process as an evaluation of the influence of the dating uncertainty on our SMB reconstruction.

3.2 Surface Mass Balance record

Combining the annual layer thickness data set with the gravimetric density best fit (published in Hubbard et al., 2013), we reconstructed the SMB record at the summit of the DIR from 1744 to 2011. Without correction for layer thinning, the mean annual layer thickness is 0.36 ± 0.02 m w.e..

We applied two corrections: the modified Dansgaard–Johnsen model and the adapted full Stokes model (Drews et al., 2015) (see Sect. 4.2) to investigate the influence of ice deformation on annual layer thicknesses, assuming a constant SMB.

Figure 6a shows the reconstructed history of annual layer thicknesses at IC12 from 1744 to 2011, without ice deformation and with the two different ice-deformation models (modified D–J model and Drews et al., 2015), which overlie each other at this scale. From now on, we will only consider the correction of Drews et al. (2015) as it is both similar to the modified D–J model and more closely guided by field measurements. As expected, annual layer thicknesses without ice deformation are underestimated in the oldest part of the ice core relative to that with ice deformation taken into account. Figure 6 (b–d) shows both the oldest and the youngest estimates to evaluate the influence of the dating uncertainty. The mean annual SMB, i.e., the mean corrected annual layer thickness, is 0.47 ± 0.02 m w.e.a⁻¹. As interannual variability is high, the 11 year running means are also shown. All curves show a clear positive trend in SMB from at least the second half of the 20th century.

Table 1 shows average SMB for three different periods (chosen mainly for comparison with previous studies) starting from the Tambora eruption (1816–2011): the last 111 years compared to the full period of time (i.e. 1900–2011 cf. 1816–1900), the last 50 years compared to the previous full period of time (i.e., 1962–2011 cf. 1816–1961), and the last 20 years compared to the previous full period of time (i.e. 1992–2011 cf. 1816–1992). From 1816 to 2011, the average SMB is 0.49 ± 0.02 m w.e. a⁻¹. For the last 111 years, the SMB is 0.55 ± 0.02 m w.e. a⁻¹, representing a 26 ± 1 % increase compared to the previous period. For the last 50 years (1962–2011), the SMB is 0.61 ± 0.01 m w.e. a⁻¹, representing a 32 ± 4 % increase compared to the previous period. For the last 20 years (1992–2011), the SMB is 0.64 ± 0.01 m w.e. a⁻¹ and the increase compared to the previous period is 32 ± 3 %.

Table 2 shows the detailed annual SMB for the last 10 years for our oldest and youngest estimates. In the oldest estimate, the highest SMB during the last 10 years occurred in 2011 and 2009, which belong to the 1 % and 3 % highest SMB years of the whole record, respectively. In the youngest estimate, 2002 is higher than 2009.

3.3 Sources of uncertainties

Surface Mass Balance reconstructed from ice cores can be characterized by substantial uncertainty (Rupper et al., 2015). The accuracy of reconstructed SMB depends on the dating accuracy, which, in our case, is determined by the oldest and youngest estimates. Also, given our vertical sampling resolution of $\delta^{18}\text{O}$, the location of summer peaks is only identifiable to a precision of 0.05 m where no other data are available, but this error only affects SMB at an annual resolution, as shown by error-bars in Fig. 6. Note also that it is very unlikely that we have overestimated the number of years due to the $\delta^{18}\text{O}$ sampling resolution, since a one-to-one correspondence subsists, in the deepest part of the core, between the $\delta^{18}\text{O}$ and the $\text{Na}^+/\text{SO}_4^-$ ratio.

SMB reconstructions are also influenced by density measurement error (2 % error) and small-scale variability in densification. The influence on SMB is very small. Callens et al. (2016) for example, used a semi-empirical model of firm compaction (Arthern et al., 2010) adjusting its parameters to fit the discrete measurements instead of using the best fit from Hubbard et al. (2013). Using the first model changes our reconstructed SMB values by
5 less than 2 %.

Average SMB on longer time periods are in all cases more robust than reconstructed annual SMB because they are less affected by uncertainties. These average estimates are also useful to reduce the influence of inter-annual variability.

Vertical strain rates also represent a potential source of error. A companion paper will be dedicated to a more
10 precise assessment of this factor using repeated borehole optical televiewer stratigraphy. However, the present study uses a field-validated strain rate model which is as close as possible to reality, and shows that using the simpler modified Dansgaard–Johnsen model changes the reconstructed SMB by maximum 0.001 m w.e. a⁻¹. Therefore, we are confident that refining the strain rate profile will not change our main conclusions.

Another possible source of error is the potential migration of the ice divide. Indeed, radar layers show SMB
15 asymmetry next to the DIR divide. However, Drews et al (2015) found that the ice divide of the DIR must have remained laterally stable for thousands of years to explain the comparatively large Raymond arches in the ice stratigraphy. Callens et al. (2016) find a similar argument by using the radar stratigraphy in the ice-rise flanks. The possibility for an ice-divide migration is therefore small. Temporal variability of SMB at certain locations can also be due to the presence of surface undulations upstream (e.g. Kaspari et al, 2004), but this effect is
20 minimised at ice divides.

3.4 Comparison with climate models

Figure 7 compares the trend in our IC12 SMB record with outputs from two atmospheric models: ERA-Interim reanalysis (Dee et al., 2009) and the CESM model. ERA-Interim shows no trend in the relatively short overlapping period (1979–2012) it covers. The ice core derived SMB correlates moderately to ERA-Interim and
25 RACMO2 (Lenaerts et al., 2014), yielding $R^2 = 0.36$ and 0.5 respectively. For a longer overlapping period, we used the output of the CESM model, although it is a freely evolving model that does not allow a direct comparison with measured data. The average SMB at Derwael in CESM (closest grid point) is too low (0.295 ± 0.061 m a⁻¹) because the orographic precipitation effect is not well simulated. However, CESM does reproduce (much of) the observed trend. Subtle small-scale variations in wind speed and direction, typically not resolved by
30 reanalyses or regional climate models, might disrupt the inter-annual variability of SMB, although we assume

that it does not influence the positive SMB trend found in the ice core record. Unfortunately, our method does not allow for an explicit partitioning of the SMB explained by precipitation as opposed to wind processes. Instead, we focus on the drivers of precipitation at the ice core site using the output of CESM (Fig. 8).

5 In anomalously high SMB years, sea ice coverage is substantially lower than average (20–40 fewer days with sea-ice cover, fig. 8) in the Southern Ocean northeast of the ice core location, which is the prevalent source region of atmospheric moisture for DIR (Lenaerts et al., 2013). This is associated with considerably higher near-surface temperatures (1–3 K). In low-SMB years (not shown), we see a reverse, but less pronounced signal, with higher sea ice fraction (10–20 days), and slightly lower temperatures at the oceanic source region of precipitation.

10 **4 Discussion**

4.1 Regional-scale variability

Output of the CESM show that, along with atmospheric circulation, sea-ice cover and near-surface temperatures have an influence on precipitation at a regional scale (Fig. 8).

Orography can also greatly affect SMB variability (Lenaerts et al., 2014). Local wind phenomena are important factors of interannual and spatial variability. Indeed, the lower correlation with ERA-Interim and RACMO2 in our study, as compared to ice cores collected on West Antarctica (Medley et al., 2013; Thomas et al., 2015) is presumably explained by the strong influence of local wind-induced snow redistribution and sublimation on the SMB on the wind-exposed ridge of the DIR (Lenaerts et al., 2014). However, Callens et al. (2016) showed that this spatial pattern has been constant for the last thousands of years. Therefore, our observed trend of increasing annual SMB is highly unlikely to be explained by a different orographic precipitation pattern caused by a change in local wind direction or strength.

20 This argument, along with the existing correlations with ERA-Interim and RACMO2, suggests that the observed trend is not limited to the DIR but that it is representative of at least the Roi Baudouin ice shelf, surrounding the DIR. More studies are needed in the area to confirm this.

25 **4.2 Continental-scale variability**

Our results show an increase in SMB on the DIR in coastal DML during the 20th and 21st centuries. This confirms studies that show a recent increase in precipitation in coastal East Antarctica on the basis of satellite data and regional climate models (Davis et al., 2005, Lenaerts et al., 2012). Using a new glacial isostatic

adjustment model, King et al. (2012) estimated that a $60 \pm 13 \text{ Gt a}^{-1}$ mass increase for the East Antarctic Ice Sheet during the last 20 years was concentrated along coastal regions, particularly in DML. However, until now, no increase had been detected in ice cores from the area. Our study is the first to detect in situ an increase in coastal Antarctic precipitation, which is expected to occur mainly in the peripheral areas at surface elevations below
5 2250 m (Krinner et al., 2007; Genthon et al., 2009).

However, not all of Antarctica would be expected to have the same SMB trend. Figure 1 and Table A1 summarize results on SMB trends from previous studies based on ice cores, extended with a few studies based on stake networks and radar. The colours of the sites indicated on Fig. 1 show the SMB change at that site. The reference period corresponds to the last ~200 years, and it is compared to two recent periods of different lengths,
10 corresponding approximately to the last ~50 years and to the last ~20 years. The exact periods are given in Table A1.

The ISMASS Committee (2004) pointed out the importance of analysing coastal records. Twenty-three of the temporal records found in the literature concern ice cores drilled less than 100 km from the coast and below 1500 m above sea level, among which 17 are located in DML. However, only two of those records cover a
15 period longer than 100 years: S100 (Kaczmarska et al., 2004) and B04 (Schlosser and Oerter, 2002). They both show a small negative trend (Fig. 1).

For the whole continent, most studies (69 % of those comparing the last ~50 years with the last ~200 years) show no significant trend (< 10 % change). For example, Isaksson et al. (1996) found <3 % change at the EPICA
20 drilling site (Amundsenisen, DML) between 1865-1965 and 1966–1991. No trend was found on most inland and coastal sites (e.g. B31, S20) in DML for the second part of the 20th century (Isaksson et al., 1999; Oerter et al. 1999, 2000; Hofstede et al., 2004; Fernandoy et al., 2010). When we consider only the studies comparing the last 20 years to the last 200 years, the percentage reporting no significant trend falls from 69 % to 46 %. The trends revealed are both positive and negative and concern the whole Antarctic continent.

25 A few studies show a decrease of more than 10 % (9 % of the studies observed this decrease during the last ~50 years and 18 % during the last ~20 years). This is the case for several inland sites in DML (e.g. Anschutz et al., 2011), but also coastal sites in this region (Kaczmarska et al., 2004: S100; Isaksson and Melvold, 2002: Site H; Isaksson et al., 1999: S20; Isaksson et al., 1996: Site E; Isaksson et al., 1999: Site M).

Twenty-one percent of the studies record an increase of >10 % of SMB starting during the last ~50 years and 36
30 % of the studies show such an increase starting during the last ~20 years. In East Antarctica, positive trends were only recorded at inland sites, e.g. in DML (Moore et al., 1991; Oerter et al., 2000), at South Pole Station (Mosley

and Thompson, 1999), Dome C (Frezzotti et al., 2005), and around Dome A (Ren et al., 2010; Ding et al., 2011). Other positive trends were found on the Antarctic Peninsula in coastal West Antarctica (Thomas et al., 2008; Aristarain et al., 2004). For some sites, the increase only started ~20 years ago (Site M: Karlof et al., 2005). Frezzotti et al. (2013) compared the sites with low SMB ($< 0.3 \text{ m w.e. a}^{-1}$) with the sites with higher SMB and found that most of the high SMB sites show an increase in SMB. However, Fig. 9 shows that coastal sites (below 1500 m a.s.l. and less than 100 km from the ice shelf) do not all behave similarly. Most of the sites with high accumulation (coastal or not) show an increase in SMB between the last ~50 years and the reference period (last ~200 years), whereas the sites with lower SMB show no trend, even if they are coastal (Fig. 9a). This figure also shows that only two other coastal sites can be used to compare the last ~200 years with the last 20 years (Fig. 9b). Comparing the last ~20 years with the last ~50 years, the increase is less important (Fig. 9c).

4.3 Causes of spatial and temporal variability

The positive temporal trend in SMB measured here and in ice cores from other areas, as well as the apparent spatial contrast, could be the result of thermodynamic forcing (temperature change), dynamic forcing (change in atmospheric circulation) or both.

Higher temperature induces higher saturation vapor pressure, generally enhancing precipitation. Oerter et al. (2000) demonstrated a correlation between temperature and SMB in DML. On longer timescales (glacial–interglacial), using ice cores and models, Frieler et al., (2015) found a correlation between temperature and SMB for the whole Antarctic continent. However, both Altnau et al. (2015) and Fudge et al. (2016) found that SMB and changes in ice $\delta^{18}\text{O}$ are not always correlated. They hypothesized that changes in synoptic circulation (cyclonic activity) have more influence than thermodynamics, especially at the coast.

In the presence of a blocking anticyclone at subpolar latitudes, an amplified Rossby wave invokes the advection of moist air (Schlosser et al., 2010; Frezzotti et al., 2013). On these rare occasions, meridional moisture transport towards the interior in DML is concentrated into atmospheric rivers. Two recent manifestations of these short-lived events, in 2009 and 2011, have led to a recent positive mass balance of the East Antarctic ice sheet (Shepherd et al., 2012; Boening et al., 2012). It was also observed in situ, at a local scale, next to the Belgian Princess Elisabeth base (72°S , 21°E) (Gorodetskaya et al., 2013; 2014). Several of these precipitation events in a single year can represent up to 50 % of the annual SMB away from the coast (Schlosser et al., 2010; Lenaerts et al., 2013). At the coast, precipitation is usually event-type, but the events occur during the whole year. However, the 2009 and 2011 events are also observed in our data as two notably higher than average SMB years (2009 and 2011, Table 2). Our record places these extreme events within a historical perspective. Despite the

fact that higher SMB years exist in the recent part of record, 2009 and 2011 are amongst the 3 % and 1 % highest SMB years of the last two centuries, respectively.

A change in climate modes could also partly explain recent changes in SMB. The Southern Annular Mode (SAM) has shifted to a more positive phase during the last 50 years (Marshall, 2003). This has led to increasing cyclonic activity, but also increasing wind speed and sublimation. Kaspari et al. (2004) also established a link between periods of increased SMB and sustained El Niño events (negative Southern Oscillation Index (SOI) anomalies) in 1991–95 and 1940–42. In our detrended dataset (not shown), mean SMB is indeed 5 % higher during 1991–95 than the long-term average and 17 % higher during 1940–42. However, high SMB is also recorded during 1973–75 (19 % higher than average) while that period is characterized by positive SOI values. Therefore, climate modes seem to have little influence (or an influence of unconstrained complexity) on inter-annual variability of SMB at IC12.

Wind ablation represents one of the largest sources of uncertainty in modelling SMB. This is an important factor generating spatial and interannual variability. Highest snowfall and highest trends in predicted snowfall are expected in the escarpment zone of the continent, due to orographic uplift (Genthon et al., 2009). For example, in the escarpment area of DML, low and medium precipitation amounts can be entirely removed by the wind, while high precipitation events lead to net positive SMB (Gorodetskaya et al., 2015). An increase in SMB coupled with an enhanced wind speed could result in increased SMB where the wind speed is low and decreased SMB in the windier areas (90 % of the Antarctic surface, Frezzotti et al., 2004). Frezzotti et al. (2013) suggested that SMB has increased at low altitude sites and on the highest ridges due to more frequent anticyclonic blocking events, but has decreased at intermediate altitudes due to stronger wind ablation in the escarpment areas. In DML, however, Altnau et al. (2015) reported a SMB increase on the plateau (coupled to an increase in $\delta^{18}\text{O}$) and a decrease on coastal sites, which they associated with a change in circulation patterns. Around Dome A, Ding et al. (2011) also reported an increase in SMB in the inland area and a recent decrease towards the coast. Their explanation is that air masses may transfer moisture inland more easily due to climate warming.

Atmospheric circulation exhibits a primary role in determining temporal and spatial SMB variability. Sea-ice and ocean surface conditions play a secondary role, and could contribute to a higher SMB in a warmer climate. A more recent study using a fully coupled climate model (Lenaerts et al., 2016) suggests that DML is the region most susceptible to an increase in snowfall in a present and future warmer climate. The snowfall increase in the coastal regions is particularly attributed to loss of sea ice cover in the Southern Atlantic Ocean, which in turn enhances atmospheric moisture uptake by evaporation. This is further illustrated in Fig. 8, which suggests that extremely high SMB years are associated with low sea ice cover. The longer exposure of open water leads to

higher near-surface temperatures and enhances evaporation and moisture availability for ice sheet precipitation (Lenaerts et al., 2016).

5 Conclusions

A 120 m ice core was drilled on the divide of the DIR, and dated back to 1759 ± 16 A.D. using $\delta^{18}\text{O}$, δD , major ion and ECM data. Due to the coastal location of the ice core, the identification of volcanic horizons is hampered by high background acidity. Therefore, we rely on a range of estimates between an oldest and a youngest depth-age scale to calculate the average SMB and temporal trends at this site and their uncertainties. The average SMB between 1816–2011 is 0.47 ± 0.02 m w.e. a^{-1} after corrections for densification and dynamic layer thinning. A 32 ± 4 % increase in SMB is reconstructed during the 20th and 21st centuries, confirming the relative trend calculated by the CESM for this area. Wind redistribution may well have a substantial impact on interannual variability of SMB at the DIR, but it is unlikely that it has an influence on the temporal trend.

The trends in SMB observed in other records all over Antarctica are spatially highly variable. In coastal East Antarctica, our study is the only to show an increase in SMB during the 20th and 21st centuries. Many studies point to a difference in the behaviour of coastal and inland sites, due to a combination of thermodynamics and dynamic processes. A combination of spatial variability in snowfall and snow redistribution by the wind explain the observed spatial variations and the poor correlation between our record and the climate reanalyses (ERA-Interim and RACMO2). Our analysis suggests that atmospheric circulation to a great extent determines SMB variability, with a potential secondary role of changes in sea ice cover. More studies are needed at other coastal sites in East Antarctica to determine how representative this result is.

Long time-series of annual SMB are scarce in coastal East Antarctica. The divide of Derwael Ice Rise is a suitable drilling site for deep drilling. It has a high SMB, and appropriate ice conditions (few thin ice layers) for paleoclimate reconstruction. According to the full Stokes model (Drews et al., 2015), drilling to 350 m could reveal at least 2000 years of a reliable climate record with high resolution, which would address one of the priority targets ("IPICS-2k array", Steig et al., 2005) of the International Partnership in Ice Core Science (IPICS).

Data Availability

Age–depth data and uncorrected SMB are available online (doi:10.1594/PANGAEA.857574).

Acknowledgements

This paper forms a contribution to the Belgian Research Programme on the Antarctic (Belgian Federal Science Policy Office), Project SD/SA/06A Constraining ice mass changes in Antarctica (IceCon). The authors wish to thank the International Polar Foundation for logistic support in the field. MP is partly funded by a grant from Fonds David et Alice Van Buuren. JTML is funded by Utrecht University through its strategic theme Sustainability, sub-theme Water, Climate and Ecosystems, and the programme of the Netherlands Earth System Science Centre (NESSC), financially supported by the Ministry of Education, Culture and Science (OCW). Ph. C. thanks the Hercules Foundation (www.herculesstichting.be/) for financing the upgrade of the stable isotope laboratory. The research leading to these results has received funding from the European Research Council under the European Community's Seventh Framework Programme (FP7/2007-2013) / ERC grant agreement 610055 as part of the Ice2Ice project. The authors also thank Irina Gorodetskaya for her helpful comments. The initial version of the manuscript has benefited from the very constructive comments and corrections of two anonymous referees and the editor.

References

- 15 Altnau, S., Schlosser, E., Isaksson, E., and Divine, D.: Climatic signals from 76 shallow firn cores in Dronning Maud Land, East Antarctica, *The Cryosphere*, 9(3), 925-944, 2015.
- Anschütz, H., Müller K., Isaksson, E., McConnell, J. R., Fischer, H., Miller, H., Albert, M., and Winther, J.-G.: Revisiting sites of the South Pole Queen Maud Land Traverses in East Antarctica: accumulation data from shallow firn cores, *J. Geophys. Res.*, 114, D24106, doi:10.1029/2009JD012204, 2009.
- 20 Anschütz, H., Sinisalo, A., Isaksson, E., McConnell, J. R., Hamran, S.-E., Bisiaux, M. M., Pasteris, D., Neumann, T. A., and Winther, J.-G.: Variation of accumulation rates over the last eight centuries on the East Antarctic Plateau derived from volcanic signals in ice cores, *J. Geophys. Res.*, 116, D20103, doi:10.1029/2011JD015753, 2011.
- Arthern, R. J., Vaughan, D. G., Rankin, A. M., Mulvaney, R., and Thomas, E. R.: In situ measurements of Antarctic snow compaction compared with predictions of models, *J. Geophys. Res.*, 115, F03011, doi:10.1029/2009JF001306, 2010.
- 25 Aristarain, A. J., Delmas, R. J., and Stievenard, M.: Ice-core study of the link between sea-salt aerosol, sea-ice cover and climate in the Antarctic Peninsula area, *Clim. Change*, 67, 63–86, 2004.

- Boening, C., Lebsack, M., Landerer, F., and Stephens, G.: Snowfall driven mass change on the East Antarctic ice sheet, *Geophys. Res. Lett.*, 39, L21501, doi:10.1029/2012GL053316, 2012.
- Bromwich, D. H., Nicolas, J. P., and Monaghan, A. J.: An assessment of precipitation changes over Antarctica and the Southern Ocean since 1989 in contemporary global reanalyses, *J. Clim.*, 24, 4189–4209, 2011.
- 5 Bromwich, D. H., Nicolas, J. P., Monaghan, A. J., Lazzara, M. A., Keller, L. M., Weidner, G. A., and Wilson, A. B.: Corrigendum: Central West Antarctica among the most rapidly warming regions on Earth. *Nature Geoscience*, 7(1), 76–76, 2014.
- Callens, D., Drews, R., Witrant, E., Philippe, M., and Pattyn, F.: Temporally stable surface mass balance asymmetry across an ice rise derived from radar internal reflection horizons through inverse modeling,
10 *J. Glaciol.*, doi:10.1017/jog.2016.41, 2016.
- Cuffey, K. M., and Paterson, W.: *The physics of glaciers*, Elsevier, 693 pp., 2010.
- Dansgaard, W., and Johnsen, S.: A flow model and a time scale for the ice core from Camp Century, Greenland, *J. Glaciol.*, 8, 215–223, 1969.
- Davis, C. H., Li, Y., McConnell, J. R., Frey, M. M., and Hanna, E.: Snowfall-driven growth in East Antarctic Ice
15 Sheet mitigates recent sea-level rise, *Science*, 308, 1898–1901, 2005.
- Ding, M., Xiao, C., Li, Y., Ren, J., Hou, S., Jin, B., and Sun, B.: Spatial variability of surface mass balance along a traverse route from Zhongshan station to Dome A, Antarctica, *J. Glaciol.*, 57, 658–666, doi:10.3189/002214311797409820, 2011.
- Drews, R., Matsuoka, K., Martín, C., Callens, D., Bergeot, N., and Pattyn, F.: Evolution of Derwael Ice Rise in
20 Dronning Maud Land, Antarctica, over the last millennia, *J. Geophys. Res., Earth Surf.*, 120, 564–579. doi: 10.1002/2014JF003246, 2015.
- Ekaykin, A. A., Lipenkov, V. Y., Kuzmina, I., Petit, J. R., Masson-Delmotte, V., and Johnsen, S. J.: The changes in isotope composition and accumulation of snow at Vostok station, East Antarctica, over the past 200 years, *Ann. Glaciol.*, 39, 569–575, 2004.
- 25 Fernandoy, F., Meyer, H., Oerter, H., Wilhelms, F., Graf, W., and Schwander, J.: Temporal and spatial variation of stable-isotope ratios and accumulation rates in the hinterland of Neumayer station, East Antarctica, *J. Glaciol.*, 56, 673–687, 2010.
- Frezzotti, M., Pourchet, M., Flora, O., Gandolfi, S., Gay, M., Urbini, S., Vincent, C., Becagli, S., Gagnani, R., Proposito, M., Severi, M., Traversi, R., Udisti, R., and Fily, M.: New estimations of precipitation and
30 surface sublimation in East Antarctica from snow accumulation measurements, *Clim. Dyn.*, 23, 803–813, doi:10.1007/s00382-00004-00462-0038500803-00813, 2004.

- Frezzotti, M., Pourchet, M., Flora, O., Gandolfi, S., Gay, M., Urbini, S., Vincent, C., Becagli, S., Gragnani, R., Proposito, M., Severi, M., Traversi, R., Udisti, R., and Fily, M.: Spatial and temporal variability of snow accumulation in East Antarctica from traverse data, *J. Glaciol.*, 51, 113–124, 2005.
- Frezzotti, M., Urbini, S., Proposito, M., Scarchilli, C., and Gandolfi, S.: Spatial and temporal variability of surface mass balance near Talos Dome, East Antarctica, *J. Geophys. Res.*, 112, F02032, doi:10.1029/2006JF000638, 2007.
- Frezzotti, M., Scarchilli, C., Becagli, S., Proposito, M., and Urbini, S.: A synthesis of the Antarctic surface mass balance during the last 800 yr, *The Cryosphere*, 7, 303–319, doi: 10.5194/tc-7-303-2013, 2013.
- Frieler, K., Clark, P. U., He, F., Buizert, C., Reese, R., Ligtenberg, S. R., van den Broeke, M.R., Winkelmann, R., and Levermann, A.: Consistent evidence of increasing Antarctic accumulation with warming, *Nat. Clim. Change*, 5, 348–352, doi: 10.1038/nclimate2574, 2015.
- Fudge, T. J., Markle, B. R., Cuffey, K. M., Buizert, C., Taylor, K. C., Steig, E. J., Waddington, E. D., Conway, H., and Koutnik, M.: Variable relationship between accumulation and temperature in West Antarctica for the past 31,000 years, *Geophys. Res. Lett.*, 43, 3795–3803, doi:10.1002/2016GL068356, 2016.
- Fujita, S., Holmlund, P., Andersson, I., Brown, I., Enomoto, H., Fujii, Y., Fujita, K., Fukui, K., Furukawa, T., Hansson, M., Hara, K., Hoshina, Y., Igarashi, M., Iizuka, Y., Imura, S., Ingvander, S., Karlin, T., Motoyama, H., Nakazawa, F., Oerter, H., Sjöberg, L. E., Sugiyama, S., Surdyk, S., Ström, J., Uemura, R., and Wilhelms, F.: Spatial and temporal variability of snow accumulation rate on the East Antarctic ice divide between Dome Fuji and EPICA DML, *The Cryosphere*, 5, 1057–1081, doi:10.5194/tc-5-1057-2011, 2011.
- Genthon, C., Krinner, G., and Castebrunet, H.: Antarctic precipitation and climate-change predictions: horizontal resolution and margin vs plateau issues, *Ann. Glaciol.*, 50(50), 55-60, 2009.
- Gorodetskaya, I. V., Van Lipzig, N. P. M., Van den Broeke, M. R., Mangold, A., Boot, W., and Reijmer, C. H.: Meteorological regimes and accumulation patterns at Utsteinen, Dronning Maud Land, East Antarctica: Analysis of two contrasting years, *J. Geophys. Res.-Atmos.*, 118, 1700–1715, doi:10.1002/jgrd.50177, 2013.
- Gorodetskaya, I. V., Tsukernik, M., Claes, K., Ralph, M. F., Neff, W. D., and Van Lipzig, N. P. M.: The role of atmospheric rivers in anomalous snow accumulation in East Antarctica, *Geophys. Res. Lett.*, 41, 6199–6206, doi:10.1002/2014GL060881, 2014.

- Gorodetskaya, I. V., Kneifel, S., Maahn, M., Van Tricht, K., Thiery, W., Schween, J. H., Mangold, A., Crewell, S., and Van Lipzig, N. P. M.: Cloud and precipitation properties from ground-based remote-sensing instruments in East Antarctica, *The Cryosphere*, 9, 285–304, doi:10.5194/tc-9-285-2015, 2015.
- 5 Hammer, C.U.: Acidity of polar ice cores in relation to absolute dating, past volcanism, and radio-echoes, *J. Glaciol.*, 25(93), 359–372, 1980.
- Hammer, C. U., Clausen, H. B., and Langway Jr, C. C.: Electrical conductivity method (ECM) stratigraphic dating of the Byrd Station ice core, Antarctica, *Ann. Glaciol.*, 20, 115–120, 1994.
- Hofstede, C. M., van de Wal, R. S. W., Kaspers, K. A., van den Broeke, M. R., Karlöf, L., Winther, J. G., Isaksson, E., Lappégard, G., Mulvaney, R., Oerther, H., and Wilhelms, F.: Firn accumulation records
10 for the past 1000 years on the basis of dielectric profiling of six firn cores from Dronning Maud Land, Antarctica, *J. Glaciol.*, 50, 279–291, 2004.
- Hubbard, B., Tison, J.-L., Philippe, M., Heene, B., Pattyn, F., Malone, T., and Freitag, J. J.: Ice shelf density reconstructed from optical televiewer borehole logging, *Geophys. Res. Lett.*, 40(22), 5882–5887, 2013.
- 15 Igarashi, M., Nakai, Y., Motizuki, Y., Takahashi, K., Motoyama, H., and Makishima, K.: Dating of the Dome Fuji shallow ice core based on a record of volcanic eruptions from AD 1260 to AD 2001, *Polar Sci.*, 5, 411–420, doi:10.1016/j.polar.2011.08.001, 2011.
- Isaksson, E., and Melvold, K.: Trends and patterns in the recent accumulation and oxygen isotope in coastal Dronning Maud Land, Antarctica: interpretations from shallow ice cores, *Ann. Glaciol.*, 35, 175–180, 2002.
- 20 Isaksson, E., Karlén, W., Gundestrup, N., Mayewski, P., Whitlow, S., and Twickler, M.: A century of accumulation and temperature changes in Dronning Maud Land, Antarctica, *J. Geophys. Res.*, 101, 7085–7094, 1996.
- Isaksson, E., van den Broeke, M. R., Winther, J.-G., Karlöf, L., Pinglot, J. F., and Gundestrup, N.: Accumulation and proxytemperature variability in Dronning Maud Land, Antarctica, determined from shallow firn
25 cores, *Ann. Glaciol.*, 29, 17–22, 1999.
- ISMSS Committee: Recommendations for the collection and synthesis of Antarctic Ice Sheet mass balance data, *Global Planet. Change*, 42, 1–15, doi:10.1016/j.gloplacha.2003.11.008, 2004.
- Jiang, S., Cole-Dai, J., Li, Y., Ferris, D.G., Ma, H., An, C., Shi, G., and Sun, B.: A detailed 2840 year record of explosive volcanism in a shallow ice core from Dome A, East Antarctica, *J. Glaciol.*, 58, 65–75,
30 doi:10.3189/2012JoG11J138, 2012.

- Kaczmarska, M., Isaksson, E., Karlöf, K., Winther, J-G, Kohler, J., Godtliobsen, F., Ringstad Olsen, L., Hofstede, C. M., van den Broeke, M. R., Van DeWal, R. S.W., and Gundestrup, N.: Accumulation variability derived from an ice core from coastal Dronning Maud Land, Antarctica, *Ann. Glaciol.*, 39, 339–345, 2004.
- 5 Karlöf, L., Winther, J. G., Isaksson, E., Kohler, J., Pinglot, J. F., Wilhelms, F., Hansson, M., Holmlund, P., Nyman, M., Pettersson, R., Stenberg, M., Thomassen, M. P. A., van der Veen, C., and van de Wal, R. S. W.: A 1500 year record of accumulation at Amundsenisen western Dronning Maud Land, Antarctica, derived from electrical and radioactive measurements on a 120 m ice core, *J. Geophys. Res.*, 105(D10), 12471–12483, doi:10.1029/1999JD901119, 2000.
- 10 Karlof, L., Isakson, E., Winther, J. G., Gundestrup, N., Meijer, H. A. J., Mulvaney, R., Pourcher, M., Hofstede, C., Lappegard, G., Petterson, R., van den Broecke, M. R., and van de Wal, R. S. W.: Accumulation variability over a small area in east Dronning Maud Land, Antarctica, as determined from shallow firn cores and snow pits: some implications for ice, *J. Glaciol.*, 51, 343–352, doi:10.3189/172756505781829232, 2005.
- 15 Kaspari, S., Mayewski, P. A., Dixon, D. A., Spikes, V. B., Sneed, S. B., Handley, M. J., and Hamilton, G. S.: Climate variability in west Antarctica derived from annual accumulation-rate records from ITASE firn/ice cores, *Ann. Glaciol.*, 39, 585–594, doi:10.3189/172756404781814447, 2004.
- King, M. A., Bingham, R. J., Moore, P., Whitehouse, P. L., Bentley, M. J., and Milne, G. A.: Lower satellite-gravimetry estimates of Antarctic sea-level contribution, *Nature*, 491, 586–589, doi:10.1038/nature11621, 2012.
- 20 Kingslake, J., R. C. A. Hindmarsh, G. Aðalgeirsdóttir, H. Conway, H. F. J. Corr, F. Gillet-Chaulet, C. Martín, E. C. King, R. Mulvaney, and H. D. Pritchard: Full-depth englacial vertical ice sheet velocities measured using phase-sensitive radar, *J. Geophys. Res.: Earth Surface*, 119(12), 2604–2618, 2014.
- Kjaer, H., Vallelonga, P., Svensson, A., Elleskov, L., Kristensen, M., Tibuleac, C., Winstrup, M., and Kipfstuhl, S.: An optical dye method for continuous determination of acidity in ice cores, *Environ. Sci. Technol.*, es-2016-00026e, *in review*.
- 25 Krinner, G., Magand, O., Simmonds, I., Genthon, C., and Dufresne, J. L.: Simulated Antarctic precipitation and surface mass balance at the end of the 20th and 21st centuries, *Clim. Dynam.* 28, 215–230, doi:10.1007/s00382-006-0177-x, 2007.

- Lenaerts, J. T. M., van den Broeke, M. R., van den Berg, W. J., van Meijgaard, E., and Munneke, P. K.: A new, high resolution surface mass balance map of Antarctica (1979–2010) based on regional climate modeling, *Geophys. Res. Lett.*, 39, L04501, doi:10.1029/2011GL050713, 2012.
- Lenaerts, J. T. M., van Meijgaard, E., van den Broeke, M. R., Ligtenberg, S. R. M., Horwath, M., and Isaksson, E.: Recent snowfall anomalies in Dronning Maud Land, East Antarctica, in a historical and future climate perspective, *Geophys. Res. Lett.*, 40, 1–5, doi : 10.1002/grl.50559, 2013.
- Lenaerts, J.T.M., Brownvan, J., den Broeke, M. R., Matsuoka, K., Drews, R., Callens, D., Philippe, M., Gorodetskaya, I., van Meijgaard, E., Reymer, C., Pattyn, F., and van Lipzig, N. P.: High variability of climate and surface mass balance induced by Antarctic ice rises, *J. Glaciol.*, 60(224): 1101, 2014.
- 10 Lenaerts, J. T. M., Vizcaino, M., Fyke, J., van Kampenhout, L., and van den Broeke, M. R.: Present-day and future Antarctic ice sheet climate and surface mass balance in the Community Earth System Model, *Clim. Dynam.*, online first, doi: 10.1007/s00382-015-2907-4, 2016.
- Levasseur, M.: Impact of Arctic meltdown on the microbial cycling of sulphur, *Nat. Geosci.*, 6, 691–700, 2013.
- Ludescher, J., Bunde, A., Franzke, C. L., and Schellnhuber, H. J.: Long-term persistence enhances uncertainty about anthropogenic warming of Antarctica, *Clim. Dyn.*, 1–9, 2015.
- 15 Magand, O., Frezzotti, M., Pourchet, M., Stenni, B., Genoni, L., and Fily, M.: Climate variability along latitudinal and longitudinal transects in east Antarctica, *Ann. Glaciol.*, 39, 351–358, doi:10.3189/172756404781813961, 2004.
- Magand, O., Genthon, C., Fily, M., Krinner, G., Picard, G., Frezzotti, M., and Ekaykin, A. A.: An up-to-date quality-controlled surface mass balance data set for the 90–180E Antarctica sector and 1950–2005 period, *J. Geophys. Res.*, 112, D12106, doi:10.1029/2006JD007691, 2007.
- 20 Marshall, G. J.: Trends in the southern annular mode from observations and reanalyses, *J. Climate*, 16, 4134–4143, 2003.
- Matsuoka, K., Hindmarsh, R. C., Moholdt, G., Bentley, M. J., Pritchard, H. D., Brown, J., Conway, H., Drews, R., Durand, G., Goldberg, D., Hattermann, T., Kingslake, J., Lenaerts, J., Martin, C., Mulvaney, R., Nicholls, K., Pattyn, F., Ross, N., Scambos, T., and Whitehouse, P.: Antarctic ice rises and rumples: their properties and significance for ice-sheet dynamics and evolution. *Earth-Sci. Rev.*, 150, 724–745, 2015.
- 25 Medley, B., Joughin, I., Das, S. B., Steig, E. J., Conway, H., Gogineni, S., Criscitiello, A. S., McConnell, J. R., Smith, B. E., van den Broeke, M. R., Lenaerts, J. T. M., Bromwich, D. H., and Nicolas, J. P.: Airborne-radar and ice-core observations of annual snow accumulation over Thwaites Glacier, West Antarctica
- 30

confirm the spatiotemporal variability of global and regional atmospheric models, *Geophys. Res. Lett.*, 40(14), 3649–3654, 2013.

- Monaghan, A. J., Bromwich, D. H., Fogt, R. L., Wang, S., Mayewski, P. A., Dixon, D. A., Ekaykin, A., Frezzotti, M., Goodwin, I., Isaksson, E., Kaspari, S. D., Morgan, V. I., Oerter, H., Van Ommen, T. D.,
5 van der Veen, C. J., and Wen, J.: Insignificant change in Antarctic snowfall since the International Geophysical Year, *Science*, 313, 827–831, doi:10.1126/science.1128243, 2006.
- Moore, J. C., Narita, H., and Maeno, N.: A continuous 770-year record of volcanic activity from East Antarctica, *J. Geophys. Res.*, 96, 17353–17359, 1991.
- Morgan, V. I., Goodwin, I. D., Etheridge, D. M., and Wookey, C. W.: Evidence for increased accumulation in
10 Antarctica, *Nature*, 354, 58–60, 1991.
- Mosley-Thompson, E., Paskievitch, J. F., Gow, A. J., and Thompson, L. G.: Late 20th century increase in South Pole snow accumulation, *J. Geophys. Res.*, 104, 3877–3886, 1999.
- Mulvaney, R., Pasteur, E.C. and Peel, D.A.: The ratio of MSA to non sea-salt sulphate in Antarctic peninsula ice cores, *Tellus*, 44b, 293-303, 1992.
- 15 Mulvaney, R., Oerter, H., Peel, D. A., Graf, W., Arrowsmith, C., Pasteur, E. C., Knight, B., Littot, G. C., and Miners, W. D: 1000-year ice core records from Berkner Island, Antarctic, *Ann. Glaciol.*, 35, 45–51, doi:10.3189/172756402781817176, 2002.
- Nishio, F., Furukawa, T., Hashida, G., Igarashi, M., Kameda, T., Kohno, M., Motoyama, H., Naoki, K., Satow, K., Suzuki, K., Morimasa, T., Toyama, Y., Yamada, T., and Watanabe, O.: Annual-layer determinations
20 and 167 year records of past climate of H72 ice core in east Dronning Maud Land, Antarctica, *Ann. Glaciol.*, 35, 471–479, 2002.
- Oerter, H., Graf, W., Wilhelms, F., Minikin, A., and Miller, H.: Accumulation studies on Amundsenisen, Dronning Maud Land, by means of tritium, DEP and stable isotope measurements: first results from the 1995/96 and 1996/97 field seasons, *Ann. Glaciol.*, 29, 1–9, doi:10.3189/172756499781820914, 1999.
- 25 Oerter, H., Wilhelms, F., Jung-Rothenhausler, F., Goktas, F., Miller, H., Graf, W., and Sommer, S.: Accumulation rates in Dronning Maud Land as revealed by DEP measurements at shallow firn cores, *Ann. Glaciol.*, 30, 27–34, 2000.
- Palmerme, C., Genthon, C., Claud, C., Kay, J. E., Wood, N. B. and L'Ecuyer, T.: Evaluation of current and projected Antarctic precipitation in CMIP5 models, *Clim.Dyn.*, online first, doi:10.1007/s00382-016-
30 3071-1, 2016.

- Parrenin, F., Dreyfus, G., Durand, G., Fujita, S., Gagliardini, O., Gillet, F., Jouzel, J., Kawamura, K., Lhomme, N., Masson-Delmotte, V., Ritz, C., Schwander, J., Shoji, H., Uemura, R., Watanabe, O., and Yoshida, N.: 1-D-ice flow modelling at EPICA Dome C and Dome Fuji, East Antarctica, *Clim. Past*, 3, 243–259, doi:10.5194/cp-3-243-2007, 2007.
- 5 Raymond, C., Weertman, B., Thompson, L., Mosley-Thompson, E., Peel, D., and Mulvaney, R.: Geometry, motion and balance of Dyer Plateau, Antarctica, *J. Glaciol.*, 42, 510–518, 1996.
- Ren, J., Li, C., Hou, S., Xiao, C., Qin, D., Li, Y., and Ding, M.: A 2680 year volcanic record from the DT-401 East Antarctic ice core, *J. Geophys. Res.*, 115, D11301, doi:10.1029/2009JD012892, 2010.
- Rignot, E., Velicogna, I., van den Broeke, M. R., Monaghan, A., and Lenaerts, J.: Acceleration of the
10 contribution of the Greenland and Antarctic ice sheets to sea level rise, *Geophys. Res. Lett.*, 38, L05503, doi:10.1029/2011GL046583, 2011.
- Roberts, J., Plummer, C., Vance, T., van Ommen, T., Moy, A., Poynter, S., Treverrow, A., Curran, M., and George, S.: A 2000-year annual record of snow accumulation rates for Law Dome, East Antarctica, *Clim. Past*, 11, 697–707, doi:10.5194/cp-11-697-2015, 2015.
- 15 Rupper, S., Christensen, W. F., Bickmore, B. R., Burgener, L., Koenig, L. S., Koutnik, M. R., Miège, C., and Forster, R. R.: The effects of dating uncertainties on net accumulation estimates from firn cores. *J. Glaciol.*, 61(225), 163–172, 2015.
- Ruth, U., Wagenbach, D., Mulvaney, R., Oerter, H., Graf, W., Pulz, H., and Littot, G.: Comprehensive 1000 year
20 climate history from an intermediate depth ice core from the south dome of Berkner Island, Antarctica: methods, dating and first results, *Ann. Glaciol.*, 39, 146–154, 2004.
- Savitzky A., and Golay, M. J. E.: Smoothing and Differentiation of Data by Simplified Least Squares Procedures. *Anal. Chem.*, 36 (8), pp 1627–1639, DOI: 10.1021/ac60214a047, 1964.
- Schlosser, E., and Oerter, H.: Shallow firn cores from Neumayer, Ekströmisén, Antarctica: a comparison of accumulation rates and stable-isotope ratios, *Ann. Glaciol.*, 35, 91–96, 2002.
- 25 Schlosser, E., Manning, K. W., Powers, J. G., Duda, M. G., Birnbaum, G., and Fujita, K.: Characteristics of high-precipitation events in Dronning Maud Land, Antarctica, *J. Geophys. Res.*, 115, D14107, doi:10.1029/2009JD013410, 2010.
- Schlosser, E., Anshütz, H., Divine, D., Martma, T., Sinisalo, A., Altnau, S., and Isaksson, E.: Recent climate tendencies on an East Antarctic ice shelf inferred from a shallow firn core network, *J. Geophys. Res.*,
30 119, 6549–6562, 2014.

- Shepherd, A., Ivins, E. R., Geruo, A., Barletta, V. R., Bentley, M. J., Bettadpur, S., Briggs, K. H., Bromwich, D. H., Forsberg, R., Galin, N., Horwath, M., Jacobs, S., Joughin, I., King, M. A., Lenaerts, J. T. M., Li, J., Ligtenberg, S. R. M., Luckman, A., Luthcke, S. B., McMillan, M., Meister, R., Milne, G., Mouginot, J., Muir, A., Nicolas, J. P., Paden, J., Payne, A. J., Pritchard, H., Rignot, E., Rott, H., Sørensen, L. S., Scambos, T. A., Scheuchl, B., Schrama, E. J. O., Smith, B., Sundal, A. V., van Angelen, J. H., van de Berg, W. J., van den Broeke, M. R., Vaughan, D. G., Velicogna, I., Wahr, J., Whitehouse, P. L., Wingham, D. J., Yi, D., Young, D., and Zwally, H. J.: A reconciled estimate of ice-sheet mass balance, *Science*, 338(6111), 1183–1189, 2012.
- 5
- Sigl, M., McConnell, J. R., Layman, L., Maselli, O., McGwire, K., Pasteris, D., Dahl-Jensen, D., Steffensen, J. P., Vinther, B., Edwards, R., Mulvaney, R., and Kipfstuhl, S.: A new bipolar ice core record of volcanism from WAIS Divide and NEEM and implications for climate forcing of the last 2000 years. *Journal of Geophysical Research: Atmospheres*, 118(3), 1151-1169, 2013.
- 10
- Sommer, S., Appenzeller, C., Röthlisberger, R., Hutterli, M. A., Stauffer, B., Wagenbach, D., Oerter, H., Wilhelms, F., Miller, H., and Mulvaney, R.: Glacio-chemical study spanning the past 2 kyr on three ice cores from Dronning Maud Land, Antarctica, 1. Annually resolved accumulation rates, *J. Geophys. Res.*, 105, 29411–29421, 2000.
- 15
- Steig, E., Fischer, H., Fisher, D., Frezzotti, M., Mulvaney, R., Taylor, K., Wolff, E.: The IPICS 2k Array: a network of ice core climate and climate forcing records for the last two millennia, <http://www.pages-igbp.org/ipics/> IPICS (International Partnership in Ice Core Science), 2005.
- 20
- Stenni, B., Caprioli, R., Cimmino, L., Cremisini, C., Flora, O., Gragnani, R., Longinelli, A., Maggi, V., and Torcini, S.: 200 years of isotope and chemical records in a firn core from Hercules Neve, northern Victoria Land, Antarctica, *Ann. Glaciol.*, 29, 106–112, 1999.
- Takahashi, H., Yokoyama, T., Igarashi, M., Motoyama, H., and Suzuki, K.: Resolution of environmental variation by detail analysis of YM85 shallow ice core in Antarctica, *Bull. Glaciol. Res.*, 27, 16–23, 2009.
- 25
- Thomas, E. R., Marshall, G. J., and McConnell, J. R.: A doubling in snow accumulation in the western Antarctic Peninsula since 1850, *Geophys. Res. Lett.*, 35, L01706, doi:10.1029/2007GL032529, 2008.
- Thomas, E. R., Hosking, J. S., Tuckwell, R. R., Warren, R.A., and Ludlow, E.C.: Twentieth century increase in snowfall in coastal West Antarctica, *Geophys. Res. Lett.*, 42, 9387–9393, doi:10.1002/2015GL065750, 2015.
- 30

- Traufetter, F., Oerter, H., Fischer, H., Weller, R., and Miller, H.: Spatio-temporal variability in volcanic sulphate deposition over the past 2 kyr in snow pits and firn cores from Amundsenisen, Antarctica., *J. Glaciol.*, 50(168), 137–146, 2004.
- 5 Turner, J., Colwell, S. R., Marshall, G. J., Lachlan-Cope, T. A., Carleton, A. M., Jones, P. D., Lagun, V., Reid, P. A. and Iagovkina, S.: Antarctic climate change during the last 50 years, *Int. J. Climatol.*, 25: 279–294, doi:10.1002/joc.1130, 2005.
- van de Berg, W. J., van den Broeke, M. R., Reijmer, C. H., and van Meijgaard, E.: Reassessment of the Antarctic SMB using calibrated output of a regional atmospheric climate model, *J. Geophys. Res.*, 111, D11104, doi:10.1029/2005JD006495, 2006.
- 15 van den Broeke, M., van de Berg, W. J., and van Meijgaard, E.: Snowfall in coastal West Antarctica much greater than previously assumed, *Geophys. Res. Lett.*, 33, L02505, doi:10.1029/2005GL025239, 2006.
- van Ommen, T. D., and Morgan, V.: Snowfall increase in coastal East Antarctica linked with southwest Western Australian drought, *Nat. Geosci.*, 3, 267–272, doi:10.1038/ngeo761, 2010.
- 20 Vaughan, D.G., Comiso, J.C., Allison, I., Carrasco, J., Kaser, G., Kwok, R., Mote, P., Murray, T., Paul, F., Ren, J., Rignot, E., Solomina, O., Steffen, K., and Zhang, T.: Observations: Cryosphere. In: *Climate Change 2013: The Physical Science Basis. Contribution of Working Group I to the Fifth Assessment Report of the Intergovernmental Panel on Climate Change* [Stocker, T.F., D. Qin, G.-K. Plattner, M. Tignor, S.K. Allen, J. Boschung, A. Nauels, Y. Xia, V. Bex and P.M. Midgley (eds.)]. Cambridge University Press, Cambridge, United Kingdom and New York, NY, USA, 2013.
- 25 Wang, Y., Ding, M., van Wessem, J., Schlosser, E., Altnau, S., van den Broeke, M., Lenaerts, J., Thomas, E., Isaksson, E., Wang, J., and Sun, W.: A comparison of Antarctic Ice Sheet surface mass balance from atmospheric climate models and in situ observations, *J. Climate*, doi:10.1175/JCLI-D-15-0642.1, early online release, 2016.
- 30 Wolff, E. W., Jones, A. E., Bauguitte, S. B., and Salmon, R. A.: The interpretation of spikes and trends in concentration of nitrate in polar ice cores, based on evidence from snow and atmospheric measurements, *Atmos. Chem. Phys.*, 8(18), 5627–5634, 2008.
- Xiao, C., Mayewski, P. A., Qin, D., Li, Z., Zhang, M., and Yan, Y.: Sea level pressure variability over the southern Indian Ocean inferred from a glaciochemical record in Princess Elizabeth Land, east Antarctica, *J. Geophys. Res.*, 109, D16101, doi:10.1029/2003JD004065, 2004.
- 35

Zhang, M., Li, Z., Ren, J., Xiao, C., Qin, D., Kang, J., and Li, J.: 250 years of accumulation, oxygen isotope and chemical records in a firn core from Princess Elizabeth Land, East Antarctica, *J. Geogr. Sci.*, 16, 23–33, doi:10.1007/s11442-006-0103-5, 2006.

Tables

Table 1. Mean SMB at IC12 for different time periods

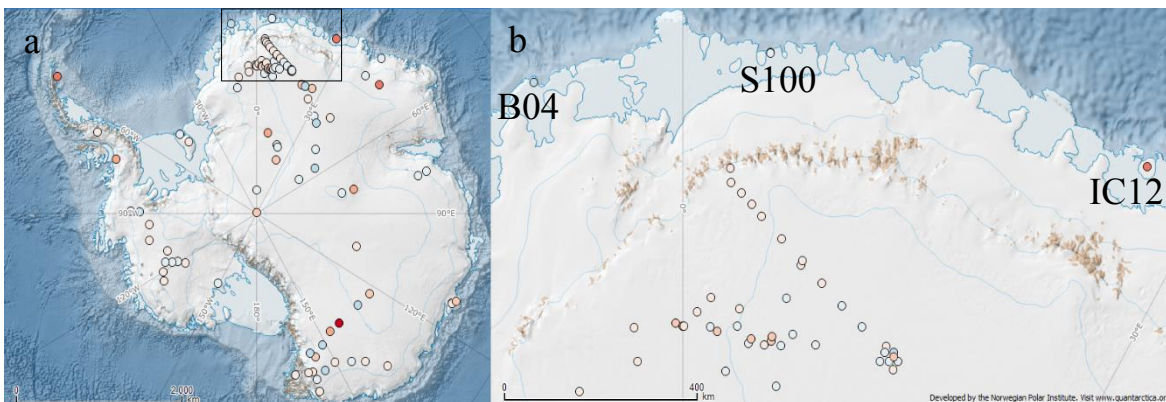
Period (years A.D.)	SMB (m w.e. a⁻¹) (oldest estimate)	SMB (m w.e. a⁻¹) (youngest estimate)	Mean SMB (m w.e. a⁻¹)
1816–2011	0.476	0.513	0.495
1816–1900	0.401	0.441	0.421
1900–2011	0.532	0.568	0.550
1816–1961	0.432	0.476	0.454
1962–2011	0.604	0.623	0.614
1816–1991	0.459	0.498	0.479
1992–2011	0.626	0.651	0.638

5 Table 2. SMB of the last 10 years from IC12 ice core (oldest and youngest estimates, see text for details)

Year (A.D.)	SMB (m w.e. a⁻¹) (oldest estimate)	SMB (m w.e. a⁻¹) (youngest estimate)
2011	0.980	0.980
2010	0.641	0.641
2009	0.824	0.824
2008	0.651	0.651
2007	0.287	0.699
2006	0.419	0.661
2005	0.661	0.681
2004	0.681	0.666
2003	0.666	0.621
2002	0.621	0.891

Figures

~1960–present vs ~1816–present



~1990–present vs ~1816–present

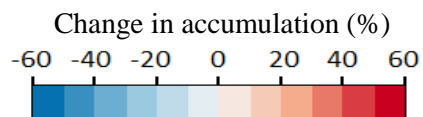
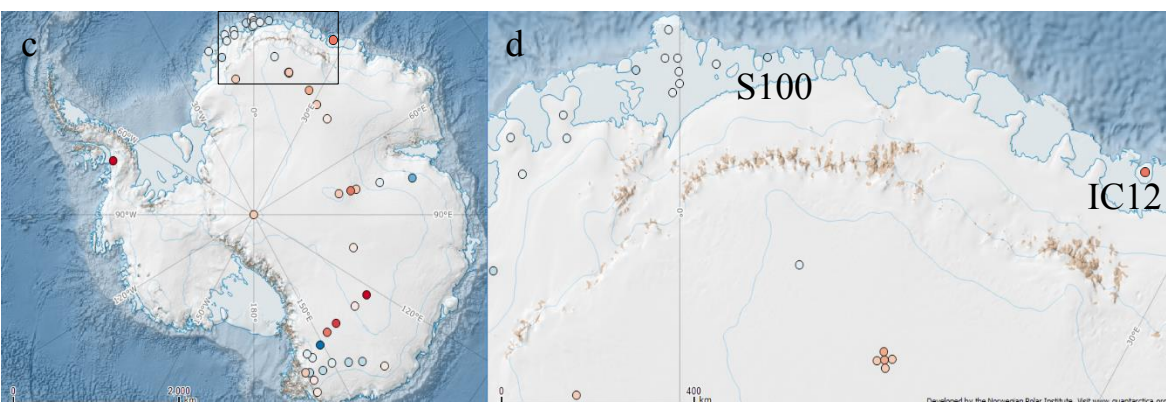


Fig. 1: Location of IC12 and other ice cores referred to herein. (a-b) Difference in mean annual SMB between the period ~1960–present and the period ~1816–present (see Table A1 for exact periods); (c-d) Same as (a-b) for the period ~1990–present compared to ~1816–present. Panels (b) and (d) are expansions of the framed areas in panels (a) and (c).

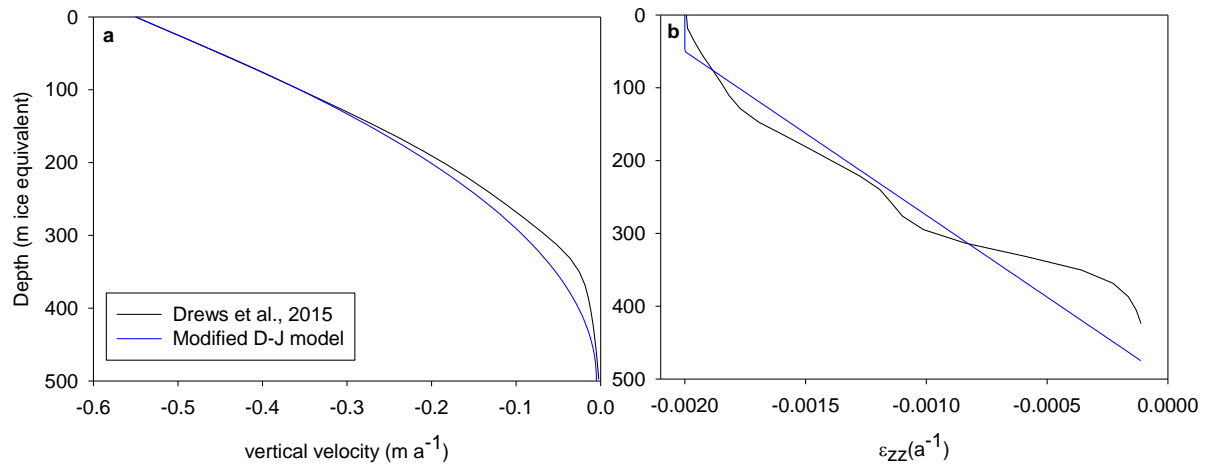


Fig. 2. (a) Vertical velocity profiles, according to the modified Dansgaard–Johnsen model (blue) and the full Stokes model (black, Drews et al., 2015). (b) Same as (a) for the vertical strain rate profiles.

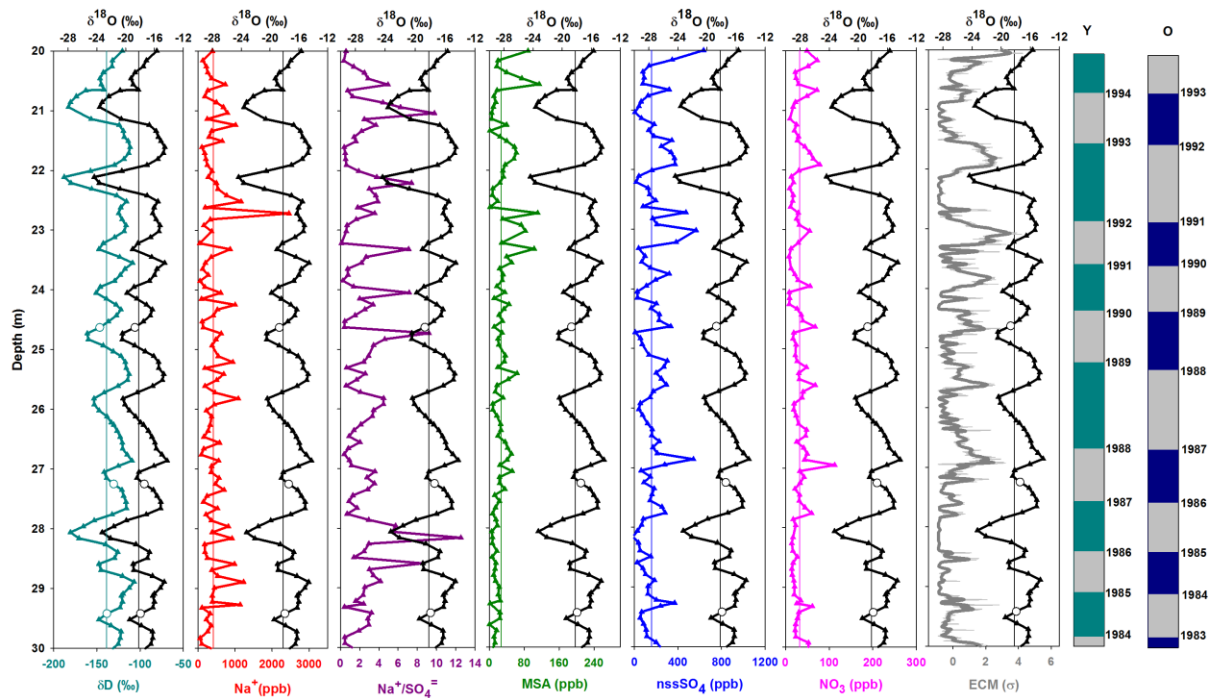


Fig. 3. A 10 m long illustrative example of how variations in stable isotopes ($\delta^{18}\text{O}$, δD), chemical species (or their ratios) and smoothed ECM (running mean, 0.1 m) are used to identify annual layers. Coloured bars on the right indicate the annual layer boundaries (middle depth of each period corresponding to above average $\delta^{18}\text{O}$ values) for the youngest (Y) and oldest (O) estimates, with 1 year difference at 20 m depth. See Fig. S1 and S2 for the whole profile. White dots in the $\delta^{18}\text{O}$ and δD profiles indicate thin ice layers identified visually in the core.

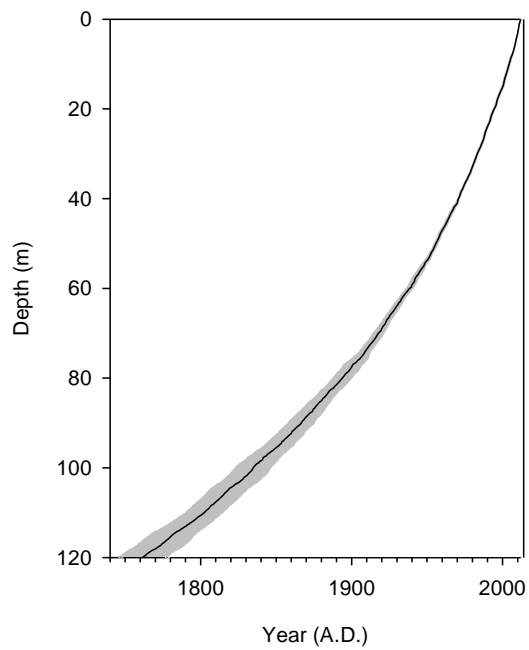


Fig. 4. Age–depth relationship for IC12 reconstructed from the relative dating process. Grey shading shows the uncertainty range between the oldest and the youngest estimates. At the bottom, the uncertainty is ± 16 years.

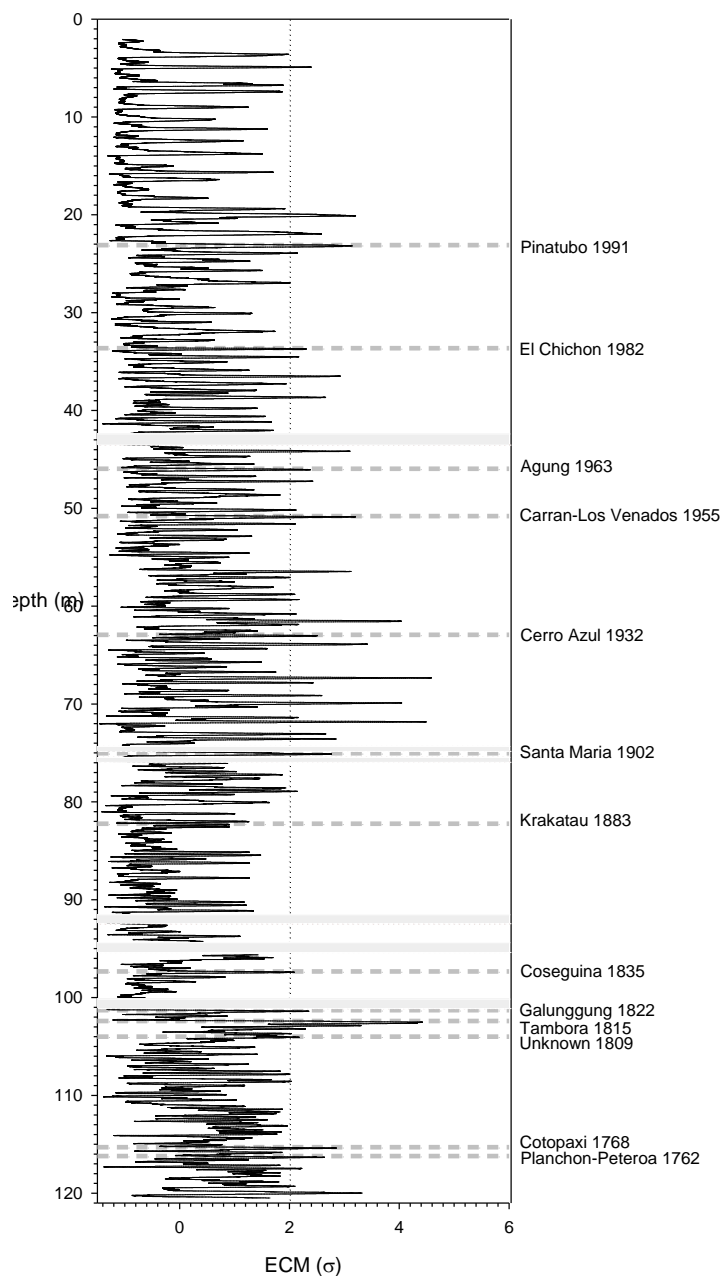


Fig. 5. Continuous record of ECM (except for 6 measurement gaps shown as grey bands). Normalized conductivity (black line) is expressed as multiple of standard deviation (σ). The 2σ threshold is shown as a dotted vertical line, and identified volcanic peaks as dashed grey horizontal lines.

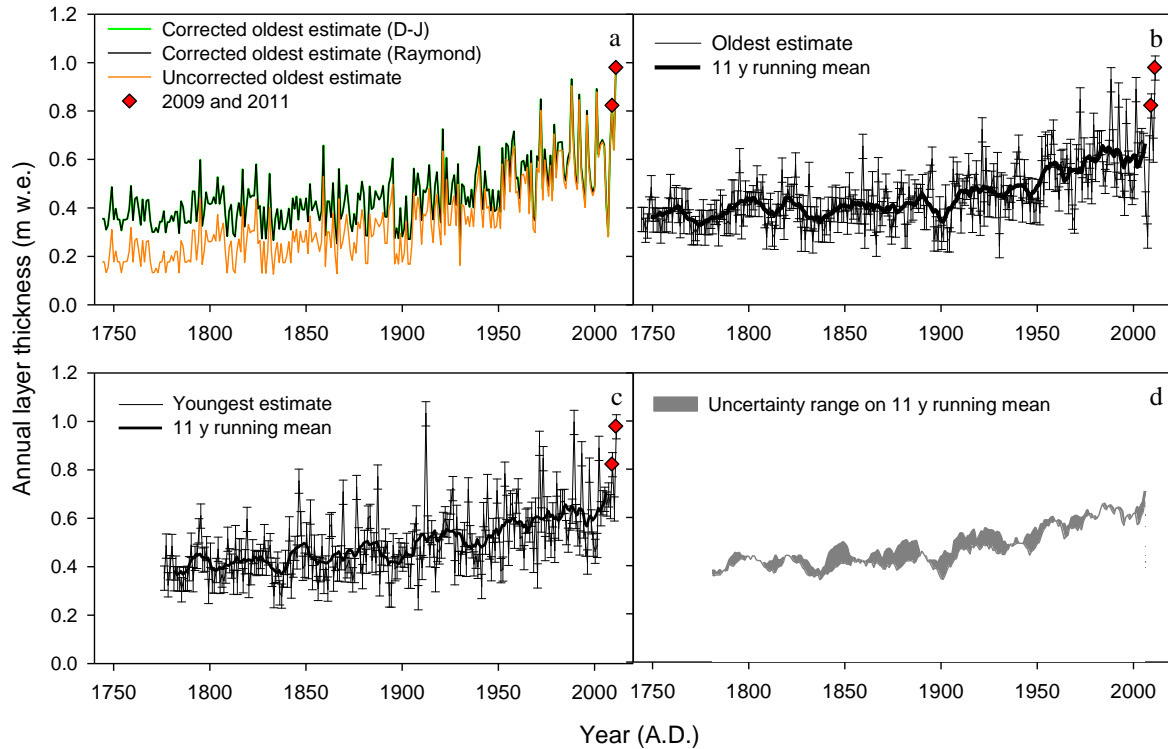


Fig. 6. Annual layer thicknesses at IC12 in m w.e.: (a) for the oldest estimate: uncorrected annual layer thickness (orange line), corrected annual layer thickness using full Stokes Drews et al. (2015) model (black line) and corrected annual layer thickness with the modified Dansgaard–Johnsen model (green line, undistinguishable from the black line at this scale); (b) corrected annual layer thickness using Drews et al. (2015) model with error bars (thin black line) and 11 year running mean (thick black line) for the oldest estimate; (c) Same as (b) for the youngest estimate (c); (d) Range of uncertainty between youngest and oldest estimates (11 year running mean). Red diamonds highlight years 2009 and 2011, discussed in the text.

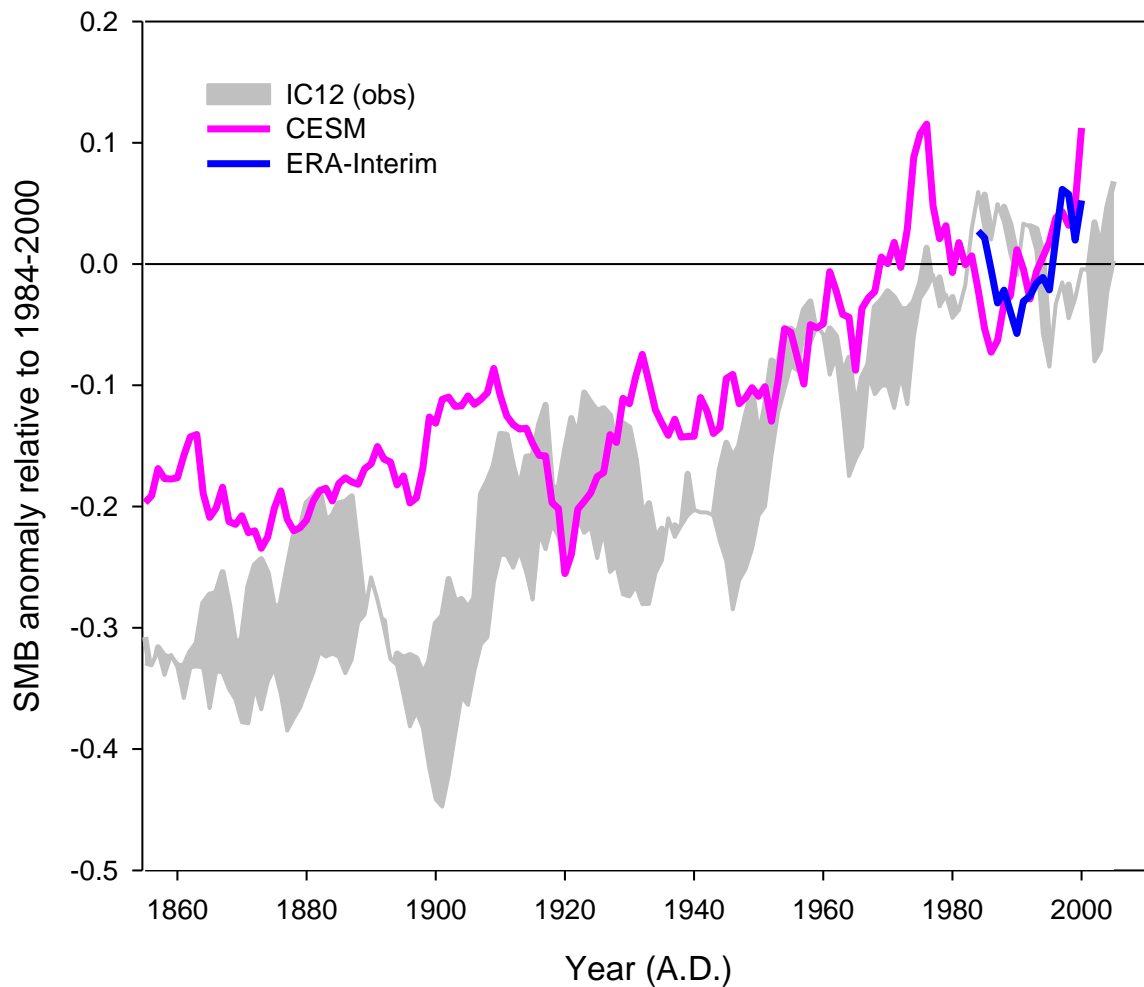


Fig. 7. Comparison between trends in IC12 record (range between youngest (upper boundary) and oldest estimate (lower boundary), shown as grey band), CESM output (pink line) and ERA-Interim reanalysis (blue line) represented as relative anomaly compared to 1979–1989 (black line), for the overlapping period 1850–2011.

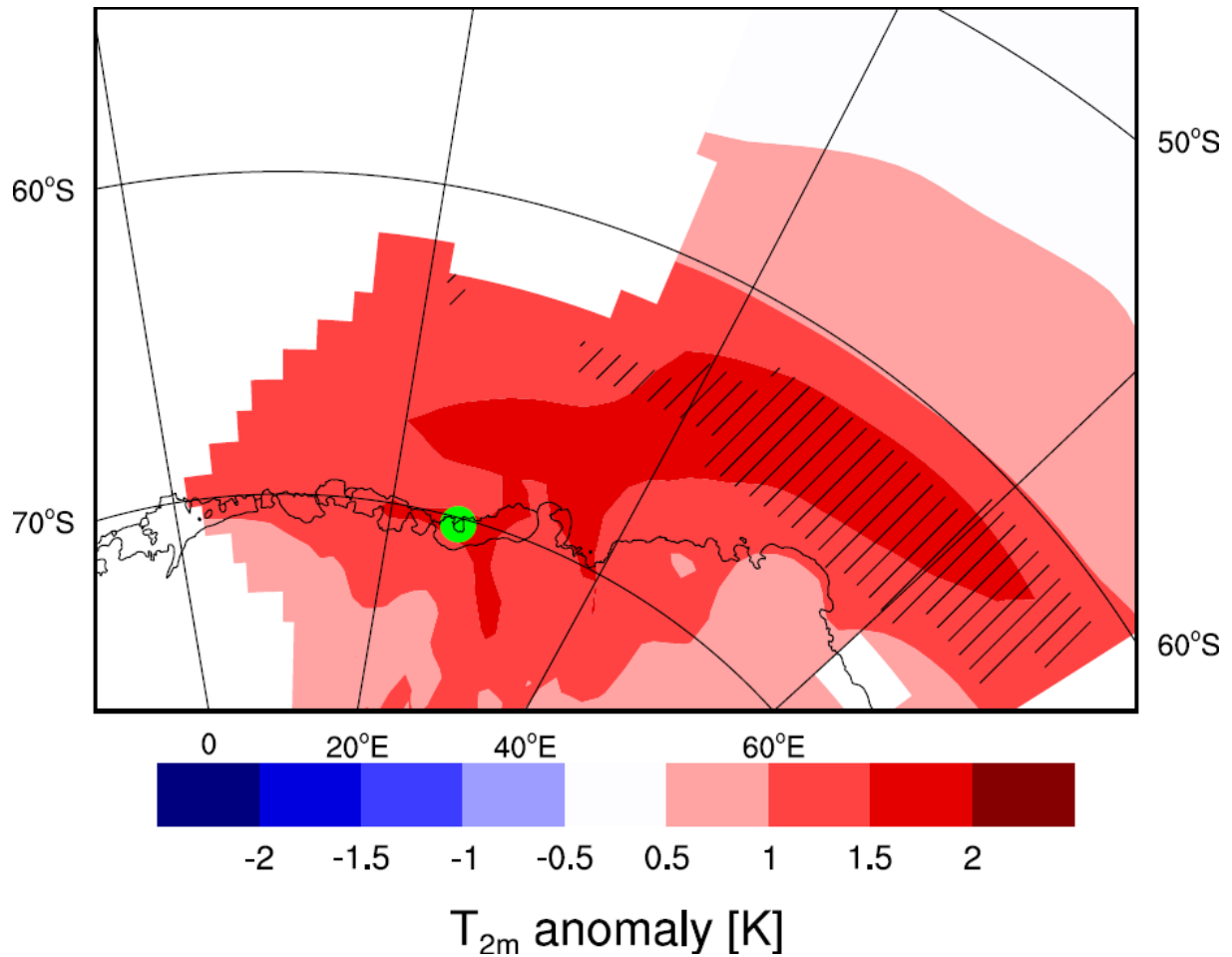


Fig. 8. Large-scale atmospheric, ocean and sea-ice anomalies in high-SMB (10 % highest) years in the CESM historical time series (1850–2005). The colours show the annual mean near-surface temperature anomaly (in °C), and the hatched areas show the anomaly in sea-ice coverage (>20 days less sea ice cover than the mean). The green dot shows the location of the ice core.

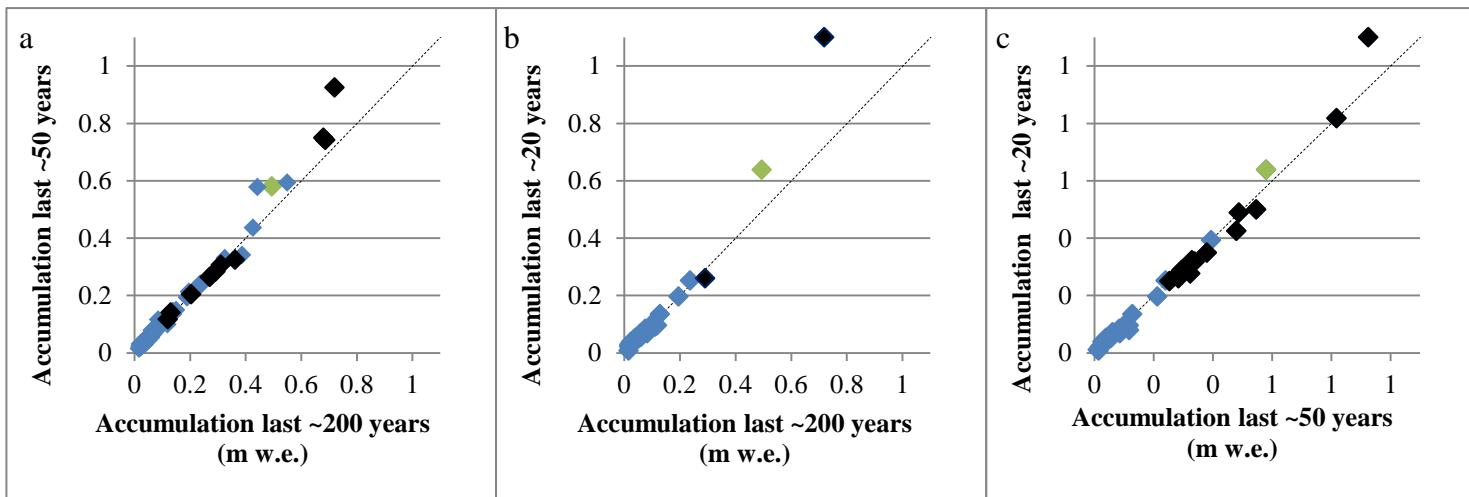


Fig. 9. Comparison of SMB between: (a) the last ~200 years and the last ~50 years; (b) the last ~200 years and the last ~20 years; (c) the last ~50 years and the last ~20 years. See Table A1 for exact periods. Coastal sites (< 1500 m a.s.l. and < 100 km away from the ice shelf) are shown in black, with the exception of our study site, IC12, which is shown in green. Inland sites are shown in blue. The 1:1 slope (0 % change) is shown as a dotted line.